Transactions of JASCOME Vol. 11 (Dec. 2011), Paper No. 21-111216 JASCOME

Vibration analysis of conical shell based on wavelet finite element method

Jiawei XIANG[1)] and Toshiro MATSUMOTO[2)]

1)Nagoya University (Furo-cho, Chikusa-ku, Nagoya, 464-8603, Japan, E-mail: xiangjw@nuem.nagoya-u.ac.jp)
2)Nagoya University (Furo-cho, Chikusa-ku, Nagoya, 464-8603, Japan, E-mail: t.matsumoto@nuem.nagoya-u.ac.jp)

A wavelet finite element method is proposed for the vibration analysis of conical shell. The scaling functions of B-spline wavelet on the interval (BSWI) is employed as the multi-scale interpolating bases. According to Hamilton's principle, the free vibration motion equations of BSWI thin truncated conical shell element will be obtained. The fundamental cause of the good performance of BSWI bases lies in that the BSWI scaling functions have the advantage of high approximation precision. Some numerical examples verify the main advantage of the proposed method is the time savings due to the substantially reduced degrees of freedom (DOFs) of BSWI method.

Key Words: Conical Shell, B-Spline Wavelet on Interval, Truncated Conical Shell Element, Modal Parameters

1. Introduction

Conical shell have a wide range of engineering applications, particularly in aerospace, marine and structural engineering. Many structures comprise at least a few components with this geometrical profile, such as turbine blades or aircraft fuselages. In practice, such components can be subjected to varying levels of dynamic stresses. However, it is difficult to obtain the closed-form solutions for conical shells with various boundary conditions. Numerical or approximate methods have been widely used to obtain the approximate solutions. For some specific situations, such as in the cases of stress concentration and high-frequency responses, traditional numerical method have drawbacks and numerously unknown DOFs will be solved. Therefore, new and reliable ways are still being developed [1-2].

Different kind of wavelet numerical methods, such as wavelet Galerkin method [3-6], wavelet finite element method [7-9] and wavelet boundary element method, etc., have proposed to solve Partial Differential Equations (PDEs) and engineering problems [10-13]. Wavelet numerical method can be viewed as a method in which the approximation functions are defined by the scaling or wavelet functions. In summary, the wavelet numerical method embody two prominent advantages [14-17]. The one is that the scale is directly upgraded using the so called two scale equations, namely, the scaling functions at different scale are employed directly to form the multi-scale approximation bases. The other is that the nesting approximation is performed using the lifting relationship between scaling and wavelet spaces, i.e. the scaling functions and wavelets at a certain scale are adopted to form the scaling function at the next scale. However, the second advantage is suit to form the adaptive wavelet Galerkin method within one element and this is very difficult to joint this adaptive element [3-6, 9].

Recently, two-dimensional Daubechies wavelet-based element for a thin plate-bending problem had been constructed in Ref. [14]. However, for Daubechies wavelet lacking of explicit expressions, present numerical integrals cannot provide desirable precision. Therefore, B-spline wavelet on the interval (BSWI) have been employed to construct 1D wavelet-based elements [15], plane elastomechanics and Mindlin plate elements [16] by using the scaling functions of BSWI. It is worth to point out that the BSWI scaling functions is modified by B-spline functions to served as complete bases in finite interval. Therefore, the stability and precision of BSWI elements are better than those of spline wavelet [17] or spline methods .

The main objective of this paper is to develop a novel vibration analysis method for thin conical shell using BSWI bases (scaling functions). This is also the extension of the present wavelet-based finite element method from static analysis to the dynamic analysis of shell structures. As we know, it need to be equipped with two degrees of freedom (DOFs)

Received Oct. 4, 2011, accepted Nov. 4, 2011

at the edge of wavelet-based element for the Hermitian interpolating , whereas it only need one DOFs for Lagrangian interpolating. We cannot using the same wavelet bases to construct the hybrid interpolating element. Therefore, we propose the hybrid scheme using both BSWI_{2j} and BSWI_{4j} scaling functions, i.e., $\mathbf{\Phi}_{2j}$ and $\mathbf{\Phi}_{4j}$. According to the kinetic energy and strain energy of the element, the Hamilton principle is employed to obtain the equations of vibration motion.

The outline of this paper is as follows. In section 2, we present a brief review of semi-orthogonal B-spline wavelet on the interval [0,1]. In section 3, BSWI scaling functions are extended to analyze the vibration of thin conical shell. Some numerical simulations and comparative investigation are presented in section 4.

2. BSWI scaling functions

Multi-resolution analysis (MRA) of BSWI on the interval [0, 1] is given by Chui, Quak and Goswami [18-19]. Suppose m and j are the order and scale of BSWI respectively, BSWI_{mj} scaling functions $\phi^j_{m,k}(\xi)$ can be calculated by

$$\phi^j_{m,k} = \begin{cases} \phi^l_{m,k}(2^{j-l}\xi), k = -m+1, \cdots, -1 \\ \phi^l_{m,2^j-m-k}(1-2^{j-l}\xi), k = 2^j - m + 1, \cdots, 2^j - 1 \\ \phi^l_{m,0}(2^{j-l}\xi - 2^{-l}k) k = 0, \cdots, 2^j - m \end{cases} \tag{1}$$

where BSWI_{m0} scaling functions are shown in Refs.[9-10]. Therefore, all the scaling functions $\mathbf{\Phi}_{mj}$ on the interval [0, 1] at the lower resolution approximation space V_j are represented by

$$\mathbf{\Phi_{mj}} = \{\phi^j_{m,-m+1}(\xi), \phi^j_{m,-m+2}(\xi), \cdots, \phi^j_{m,2^j-1}(\xi)\} \tag{2}$$

Obviously, there are $m-1$ boundary scaling functions at each end point and $2^j - m + 1$ inner scaling functions. The total scaling functions at interval [0, 1] are $2^j + m - 1$. Fig. 1 shows all the scaling functions $\mathbf{\Phi}_{43}$ and $\mathbf{\Phi}_{23}$ for BSWI_{43} and BSWI_{23}, respectively.

3. Vibration analysis of thin conical shell

For an axisymmetric conical shell, the displacement of a point on the neutral surface is uniquely determined by two components u and w in the tangential and normal directions, respectively. Fig.2 shows the layout of nodes and the corresponding degrees of freedom (DOFs) for thin conical shell. $u - w$ and $\overline{u} - \overline{w}$ are the local and global coordinate systems, respectively. The elemental length is l_e . If u and w are interpolated by BSWI_{2j} and BSWI_{4j} respectively, each element possesses $n(n = 2^j + 1)$ nodes. Both the edge node 1 and n are equipped with three DOFs, i.e., $u_i, w_i, \beta_i (i = 1, 2^j + 1)$. However, at each inner node, only the axial and radial displacements will be prescribed, i.e.,

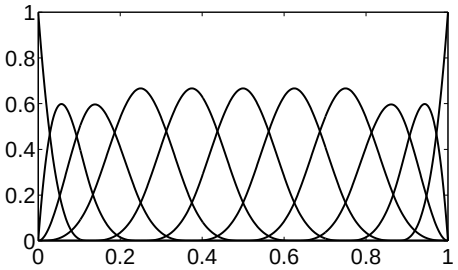

(a) $\mathbf{\Phi}_{43}$

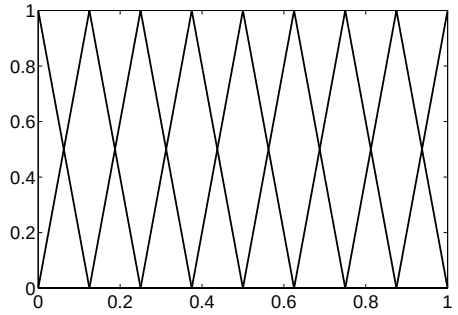

(b) $\mathbf{\Phi}_{23}$

Fig. 1 BSWI scaling functions $\mathbf{\Phi}_{43}$ and $\mathbf{\Phi}_{23}$

$u_i, w_i (i = 2, \cdots, 2^j)$. Therefore, the total DOFs of element are $2^{j+1} + 4$.

The kinetic energy T_e and strain energy U_e of the complete element are [20]

$$T_e = \frac{1}{2}\int_{\Omega_e} \rho\{(\frac{\mathrm{d}u}{\mathrm{d}t})^2 + (\frac{\mathrm{d}w}{\mathrm{d}t})^2\}\mathrm{d}\Omega_e \tag{3}$$

and

$$U_e = \frac{1}{2}\int_{\Omega_e} (\boldsymbol{\varepsilon}^{(m)})^{\mathrm{T}}\mathbf{D}^{(m)}\boldsymbol{\varepsilon}^{(m)})\mathrm{d}\Omega_e + \frac{1}{2}\int_{\Omega_e} (\boldsymbol{\varepsilon}^{(b)})^{\mathrm{T}}\mathbf{D}^{(b)}\boldsymbol{\varepsilon}^{(b)})\mathrm{d}\Omega_e \tag{4}$$

respectively, where (m) denotes membrane situation and (b) denotes bending situation, Ω_e is the elemental solving domain. The generalized strain and elasticity matrices are

$$\boldsymbol{\varepsilon}^{(m)} = \begin{Bmatrix} \varepsilon_s \\ \varepsilon_\theta \end{Bmatrix} = \begin{Bmatrix} \frac{\mathrm{d}u}{\mathrm{d}s} \\ \frac{1}{r}(u\sin\alpha + w\cos\alpha) \end{Bmatrix} \tag{5}$$

$$\boldsymbol{\varepsilon}^{(b)} = \begin{Bmatrix} \kappa_s \\ \kappa_\theta \end{Bmatrix} = \begin{Bmatrix} -\frac{\mathrm{d}^2 w}{\mathrm{d}s^2} \\ -\frac{\sin\alpha}{r}\frac{\mathrm{d}w}{\mathrm{d}s} \end{Bmatrix} \tag{6}$$

$$\mathbf{D}^{(m)} = k_0 \begin{bmatrix} 1 & \mu \\ \mu & 1 \end{bmatrix} \tag{7}$$

$$\mathbf{D}^{(b)} = D_0 \begin{bmatrix} 1 & \mu \\ \mu & 1 \end{bmatrix} \tag{8}$$

in which $k_0 = Et/(1-\mu^2)$, $D_0 = Et^3/(12(1-\mu^2))$, μ is Possion's ratio, E is Young's modulus, t is the thickness of shell, r is the tangential coordinate of a point on the neutral surface, and α is the cone angle.

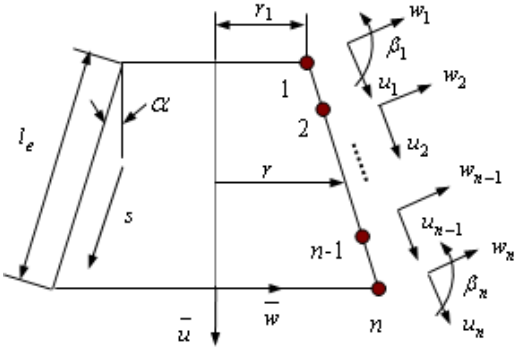

Fig. 2 BSWI thin truncated conical shell element

In order to impose the continuity and compatibility of the displacements at the interface between neighboring elements, and to introduce the boundary condition conveniently, the stiffness and mass matrices should be transformed from wavelet space into physical space. Therefore, we introduce different type of transformation matrices [15].

u and w can be interpolated independently by BSWI_{2j} and BSWI_{4j} scaling functions as

$$\begin{cases} u = \mathbf{\Phi}_{2j}\mathbf{T}_m^e\mathbf{u}^e \\ w = \mathbf{\Phi}_{4j}\mathbf{T}_b^e\mathbf{w}^e \end{cases} \tag{9}$$

where interpolation scaling functions are

$$\begin{cases} \mathbf{\Phi}_{2j} = \{\phi_{2,-1}^j(\xi), \phi_{2,0}^j(\xi)\cdots, \phi_{2,2^j-1}^j(\xi)\} \\ \mathbf{\Phi}_{4j} = \{\phi_{4,-3}^j(\xi), \phi_{4,-2}^j(\xi)\cdots, \phi_{4,2^j-1}^j(\xi)\} \end{cases} \tag{10}$$

The corresponding transformation matrices are [15]

$$\begin{cases} \mathbf{T}_m^e = ([\mathbf{\Phi}_{2j}^{\mathrm{T}}(\xi_1), \mathbf{\Phi}_{2j}^{\mathrm{T}}(\xi_2), \cdots, \mathbf{\Phi}_{2j}^{\mathrm{T}}(\xi_n)]^{\mathrm{T}})^{-1} \\ \mathbf{T}_b^e = ([\mathbf{\Phi}_{4j}^{\mathrm{T}}(\xi_1), \frac{1}{l_e}\frac{\mathrm{d}\mathbf{\Phi}_{4j}^{\mathrm{T}}(\xi_1)}{\mathrm{d}\xi}, \cdots, \mathbf{\Phi}_{4j}^{\mathrm{T}}(\xi_{n-1}), \frac{1}{l_e}\frac{\mathrm{d}\mathbf{\Phi}_{4j}^{\mathrm{T}}(\xi_n)}{\mathrm{d}\xi}]^{\mathrm{T}})^{-1} \end{cases} \tag{11}$$

and also the corresponding DOFs in local coordinate system are

$$\begin{cases} \mathbf{u}^e = \{u(s_1), u(s_2), \cdots, u(s_n)\}^{\mathrm{T}} \\ \mathbf{w}^e = \{w(s_1), \frac{\mathrm{d}w(s_1)}{\mathrm{d}s}, w(s_2), w(s_3), \cdots, w(s_{n-1}), w(s_n), \frac{\mathrm{d}w(s_n)}{\mathrm{d}s}\}^{\mathrm{T}} \end{cases} \tag{12}$$

Substituting Eqs.(5)$\sim$ (11) into Eqs.(3) and (4), according to Hamilton's principle [20] to the Lagrangian function $U_e - T_e$, the equations of free vibration motion of BSWI thin truncated conical shell element is obtained as

$$\left(\begin{bmatrix} \mathbf{K}^{e,1} & \mathbf{K}^{e,2} \\ \mathbf{K}^{e,3} & \mathbf{K}^{e,4} \end{bmatrix} - \omega^2 \begin{bmatrix} \mathbf{M}^{e,1} & 0 \\ 0 & \mathbf{M}^{e,2} \end{bmatrix}\right) \begin{bmatrix} \mathbf{u}^e \\ \mathbf{w}^e \end{bmatrix} = 0 \tag{13}$$

where $\mathbf{K}^{e,1}$,$\mathbf{K}^{e,2}$, $\mathbf{K}^{e,3}$, $\mathbf{K}^{e,4}$, $\mathbf{M}^{e,1}$, and $\mathbf{M}^{e,2}$ are

$$\mathbf{K}^{e,1} = k_0\{\mathbf{A}_1^{11} + \mu\sin\alpha(\mathbf{A}_1^{01} + \mathbf{A}_1^{10}) + \sin^2\alpha\mathbf{A}_1^{00}\} \tag{14}$$

$$\mathbf{K}^{e,2} = k_0\{\mu\cos\alpha\mathbf{A}_{12}^{10} + \sin\alpha\cos\alpha\mathbf{A}_{12}^{00}\} \tag{15}$$

$$\mathbf{K}^{e,3} = (\mathbf{K}^{e,2})^{\mathrm{T}} \tag{16}$$

$$\mathbf{K}^{e,4} = D_0\{\mathbf{A}_2^{22} + \mu\sin\alpha(\mathbf{A}_2^{21} + \mathbf{A}_2^{12}) + \sin^2\alpha\mathbf{A}_2^{11}\} + k_0\cos^2\alpha\mathbf{A}_2^{00} \tag{17}$$

$$\mathbf{M}^{e,1} = 2\pi l_e\rho t(\mathbf{T}_m^e)^{\mathrm{T}}[\int_0^1 r\mathbf{\Phi}_{2j}^{\mathrm{T}}\mathbf{\Phi}_{2j}\mathrm{d}\xi](\mathbf{T}_m^e) \tag{18}$$

$$\mathbf{M}^{e,2} = 2\pi l_e\rho t(\mathbf{T}_b^e)^{\mathrm{T}}[\int_0^1 r\mathbf{\Phi}_{4j}^{\mathrm{T}}\mathbf{\Phi}_{4j}\mathrm{d}\xi](\mathbf{T}_b^e) \tag{19}$$

in which ρ is the density of the material, ω is the angular frequency, t is the thickness of the shell. The radius r has to be expressed as a function of s, and the integral terms in Eqs. (14) $\sim$ (17) are calculated by

$$\mathbf{A}_1^{11} = \frac{2\pi}{l_e}(\mathbf{T}_m^e)^{\mathrm{T}}[\int_0^1 r\frac{\mathrm{d}\mathbf{\Phi}_{2j}^{\mathrm{T}}}{\mathrm{d}\xi}\frac{\mathrm{d}\mathbf{\Phi}_{2j}}{\mathrm{d}\xi}\mathrm{d}\xi]\mathbf{T}_m^e \tag{20}$$

$$\mathbf{A}_1^{01} = 2\pi(\mathbf{T}_m^e)^{\mathrm{T}}[\int_0^1 \mathbf{\Phi}_{2j}^{\mathrm{T}}\frac{\mathrm{d}\mathbf{\Phi}_{2j}}{\mathrm{d}\xi}\mathrm{d}\xi]\mathbf{T}_m^e \tag{21}$$

$$\mathbf{A}_1^{10} = (\mathbf{A}_1^{01})^{\mathrm{T}} \tag{22}$$

$$\mathbf{A}_1^{00} = 2\pi l_e(\mathbf{T}_m^e)^{\mathrm{T}}[\int_0^1 \frac{1}{r}\mathbf{\Phi}_{2j}^{\mathrm{T}}\mathbf{\Phi}_{2j}\mathrm{d}\xi]\mathbf{T}_m^e \tag{23}$$

$$\mathbf{A}_{12}^{10} = 2\pi(\mathbf{T}_m^e)^{\mathrm{T}}[\int_0^1 \frac{\mathrm{d}\mathbf{\Phi}_{2j}^{\mathrm{T}}}{\mathrm{d}\xi}\mathbf{\Phi}_{4j}\mathrm{d}\xi]\mathbf{T}_b^e \tag{24}$$

$$\mathbf{A}_{12}^{00} = 2\pi l_e(\mathbf{T}_m^e)^{\mathrm{T}}[\int_0^1 \mathbf{\Phi}_{2j}^{\mathrm{T}}\mathbf{\Phi}_{4j}\mathrm{d}\xi]\mathbf{T}_b^e \tag{25}$$

$$\mathbf{A}_2^{00} = 2\pi l_e(\mathbf{T}_b^e)^{\mathrm{T}}[\int_0^1 \frac{1}{r}\mathbf{\Phi}_{4j}^{\mathrm{T}}\mathbf{\Phi}_{4j}\mathrm{d}\xi]\mathbf{T}_b^e \tag{26}$$

$$\mathbf{A}_2^{22} = \frac{2\pi}{l_e^3}(\mathbf{T}_b^e)^{\mathrm{T}}[\int_0^1 r\frac{\mathrm{d}^2\mathbf{\Phi}_{4j}^{\mathrm{T}}}{\mathrm{d}\xi^2}\frac{\mathrm{d}^2\mathbf{\Phi}_{4j}}{\mathrm{d}\xi^2}\mathrm{d}\xi]\mathbf{T}_b^e \tag{27}$$

$$\mathbf{A}_2^{21} = \frac{2\pi}{l_e^2}(\mathbf{T}_b^e)^{\mathrm{T}}[\int_0^1 \frac{\mathrm{d}^2\mathbf{\Phi}_{4j}^{\mathrm{T}}}{\mathrm{d}\xi^2}\frac{\mathrm{d}\mathbf{\Phi}_{4j}}{\mathrm{d}\xi}\mathrm{d}\xi]\mathbf{T}_b^e \tag{28}$$

$$\mathbf{A}_2^{12} = (\mathbf{A}_2^{21})^{\mathrm{T}} \tag{29}$$

$$\mathbf{A}_2^{11} = \frac{2\pi}{l_e}(\mathbf{T}_b^e)^{\mathrm{T}}[\int_0^1 \frac{1}{r}\frac{\mathrm{d}\mathbf{\Phi}_{4j}^{\mathrm{T}}}{\mathrm{d}\xi}\frac{\mathrm{d}\mathbf{\Phi}_{4j}}{\mathrm{d}\xi}\mathrm{d}\xi]\mathbf{T}_b^e \tag{30}$$

The elemental physical DOFs in the local coordinate system are

$$\mathbf{a}^e = \{u_1, w_1, \frac{\mathrm{d}w_1}{\mathrm{d}s}, u_2, w_2, \cdots, u_{n-1}, w_{n-1}, u_n, w_n, \frac{\mathrm{d}w_n}{\mathrm{d}s}\}^{\mathrm{T}} \tag{31}$$

and the elemental physical DOFs in the global coo system are

$$\bar{\mathbf{a}}^e = \{\bar{u}_1, \bar{w}_1, \frac{\mathrm{d}\bar{w}_1}{\mathrm{d}s}, \bar{u}_2, \bar{w}_2, \cdots, \bar{u}_{n-1}, \bar{w}_{n-1}, \bar{u}_n, \bar{w}_n,$$

The DOFs transformation equations from the gl ordinate system to the local coordinate system can pressed as

$$\mathbf{a}^e = \mathbf{S}^e \bar{\mathbf{a}}^e$$

where the transformation matrix is

$$\mathbf{S}^e = \begin{bmatrix} \boldsymbol{\lambda}_1 & & & & \\ & \boldsymbol{\lambda}_2 & & & \\ & & \ddots & & \\ & & & \boldsymbol{\lambda}_{n-1} & \\ & & & & \boldsymbol{\lambda}_n \end{bmatrix} \tag{34}$$

in which the transformation sub-matrices for edge node are

$$\boldsymbol{\lambda}_i = \begin{bmatrix} \cos\alpha & \sin\alpha & 0 \\ -\sin\alpha & \cos\alpha & 0 \\ 0 & 0 & 1 \end{bmatrix} (i = 1, n) \tag{35}$$

and the transformation submatrices for inner node are

$$\boldsymbol{\lambda}_i = \begin{bmatrix} \cos\alpha & \sin\alpha \\ -\sin\alpha & \cos\alpha \end{bmatrix} (i = 2, 3, \cdots, n-1) \tag{36}$$

According to the elemental physical DOFs (see Eq. (31)), the location of free vibration motion equations Eq.(13) can be changed and the corresponding elemental stiffness matrix $\mathbf{K}^e$ and mass matrix $\mathbf{M}^e$ will be obtained. Therefore, in global coordinate system, the free vibration frequency equations is

$$|(\mathbf{S}^e)^{\mathrm{T}}\mathbf{K}^e(\mathbf{S}^e) - \omega^2(\mathbf{S}^e)^{\mathrm{T}}\mathbf{M}^e(\mathbf{S}^e)| = 0 \tag{37}$$

4. Numerical simulation

In order to verify the validity and advantages of the present vibration analysis method using BSWI truncated conical shell elements in the problems of axisymmestric shells, one typical numerical example is illustrated. The combination of BSWI scaling functions $\mathbf{\Phi}_{23}$ of BSWI_{23} and $\mathbf{\Phi}_{43}$ of BSWI_{43} (it can be simply abbreviated as BSWI_{2343} bases) to interpolate membrane and bending situations respectively. For simplicity, the units of all parameters are omitted.

A combined conical shell with two different boundary conditions, i.e., clamped at the left edge and at both of the left and right edges. The geometry is shown in Fig.3, the geometry and material parameters are assumed as $L = 50$, $t = 1$, $\alpha = 15^\circ$, $r = 50$, $E = 10^5$, and $\rho = 1$, respectively.

We adopt 8 BSWI_{2343} thin truncated conical shell elements with 139 DOFs) and 240 traditional elements with 964

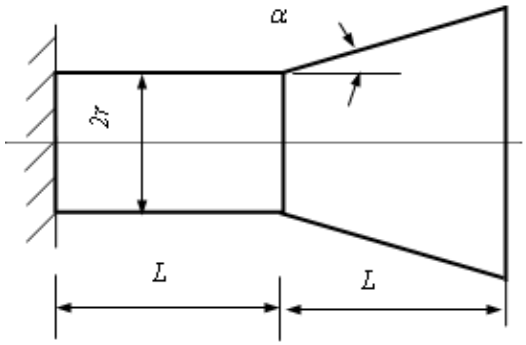

Fig. 3 Clamped combined conical shell

DOFs (SHELL 61 element in commercial software ANSYS, where each element has two points and each point equipped with three displacements, i.e., u, v and w) and one rotation β) respectively to analyze the shell. The results for the frequencies of the shell clamped at the left edge and at both the left and right edges are shown in Tables 1 and 2, respectively. The small relative error indicates a good performance of BSWI scaling functions for the dynamic analysis of conical shell. Figs. 4 and 5 show some mode shapes calculated by BSWI method (different type of dots show in Figs. 4 and 5) and those by the traditional elements (solid lines show in Figs. 4 and 5) for the shell clamped at the left edge and at both the left and right edges, respectively. In view of the overall behavior, the mode shapes computed by the present method are in reasonably good agreement with those by the traditional method. Moreover, to obtain the same approximation precision, the DOFs of traditional SHELL 61 element have to be almost 7 times of that of the 8 BSWI_{2343} thin truncated conical shell elements. It is worth pointing out that because only two displacement u and w, and one rotation β are considered in the present method, some orders of natural frequencies and mode shapes along the direction v are not available by the present method.

The numerical results presented in this paper demonstrated the validity of the present method. The main advantage of the proposed method is the time savings due to the reduced DOFs of BSWI method. The fundamental cause of the good performance of BSWI bases lies in the BSWI scaling functions have the advantages of high approximation precision.

5. Conclusions

The vibration analysis method for the thin conical shells are successfully proposed using the combination of BSWI_{2j} and BSWI_{4j} scaling functions $\mathbf{\Phi}_{2j}$ and $\mathbf{\Phi}_{4j}$. Numerical example testified the validity of wavelet-based method . The proposed wavelet-based vibration analysis method can also

Table 1 Frequencies comparison of BSWI and traditional elements [Hz]

Order	Shell61 element	BSWI element	Error/%
1	0.40944	–	–
2	0.6401	0.64016	0.009
3	0.79498	0.79543	0.057
4	0.87802	0.87881	0.090
5	0.94506	0.94548	0.044
6	0.99285	0.99324	0.039
7	1.044	1.0454	0.134
8	1.0772	1.0781	0.084
9	1.1427	1.1443	0.140
10	1.2659	1.269	0.245
11	1.4191	1.4232	0.289
12	1.4379	–	–
13	1.5998	1.6059	0.381
14	1.843	1.8516	0.467
15	2.1153	2.1263	0.520
16	2.3989	–	–
17	2.4304	2.4438	0.551
18	2.4808	2.4859	0.206
19	2.8098	2.8295	0.701
20	3.1629	3.1902	0.863

Table 2 Frequencies comparison of BSWI and traditional elements [Hz]

Order	Shell61 element	BSWI element	Error/%
1	0.87055	0.87083	0.0322
2	0.9242	0.92467	0.051
3	0.9915	0.99177	0.027
4	1.0346	1.0353	0.068
5	1.0393	–	–
6	1.0503	1.0511	0.076
7	1.1333	1.135	0.150
8	1.2598	1.2625	0.214
9	1.4033	1.407	0.264
10	1.6016	1.6068	0.325
11	1.6824	1.6827	0.018
12	1.8474	1.855	0.411
13	1.9294	–	–
14	2.1258	2.1363	0.494
15	2.4393	2.4536	0.586
16	2.7554	2.7731	0.642
17	2.9178	–	–
18	3.1464	3.1687	0.709
19	3.3212	3.33	0.265
20	3.6135	3.6436	0.833

be extended to the analysis of dynamic response or wave propagation in thin conical shell.

Acknowledgements

The authors are grateful to the support of the Japan Society for the Promotion of Science (ID: P11052). This work is also supported by the projects of Natural Science Foundation of China (No. 51175097).

References

(1) J. Zhou and Y. Lei, Asymptotic transfer function analysis of conical shells, *AIAA J.*, **36**(1998), pp. 848-854.

(2) K.Y. Lam, H. Li, T.Y. Ng and C.F. Chua, Generalized differential quadrature method for the free vibration of truncated conical planels, *J. Sound Vibr.*, **251**(2002), pp. 329-348.

(3) L.Lazaar, P. Ponenti, J. Liandrat and P. Tchamitchian, Wavelet algorithms for numerical resolution of partial differential equations, *Comput. Methods Appl. Mech. Engrg.*, **116** (1994), pp. 309-314.

(4) K. Amaratunga and R. Sudarshan, Multiresolution modeling with operator-customized wavelets derived from finite elements, *Comput. Methods Appl. Mech. Engrg.*, **195** (2006), pp. 2509-2532.

(5) R. Sudarshan, K. Amaratunga and T. Gratsch, A combined approach for goal-oriented error estimation and adaptivity using operator-customized finite element wavelets, *Int. J. Num. Meth. Engng.*, **66** (2006), pp. 1002-1035.

(6) Y.H. Zhou, J. Zhou, A modified wavelet approximation of deflections for solving PDEs of beams and square thin plates, *Finite Elem. Anal. Des.* **44** (2008), pp. 773-783.

(7) J.K. Ko, A.J. Kurdila and M.S. Pilant, Triangular wavelet based finite elements via multivalued scaling equations, *Comput. Methods Appl. Mech. Engrg.*, **146**(1997), pp. 1-17.

(8) L.M.S. Castro and J.A.T.D. Freitas, Wavelets in hybrid-mixed stress elements, *Comput. Methods Appl. Mech. Engrg.*, **190** (2001), pp. 3977-3998.

(9) S.Beuchler, Wavelet solvers for hp-FEM discretizations in 3D using hexahedral elements, *Comput. Methods Appl. Mech. Engrg.*, **198** (2009), pp. 1138-1148.

(10) K. Abe, K. Koro and K Itami, An h-hierarchical Galerkin BEM using Haar wavelets, *Eng. Anal. Bound.*

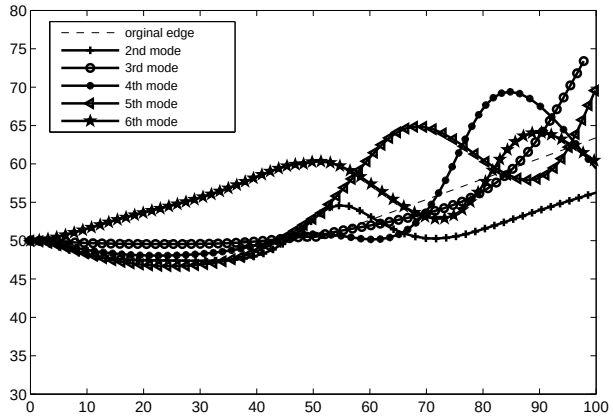

Fig. 4 The comparison of lower mode shapes

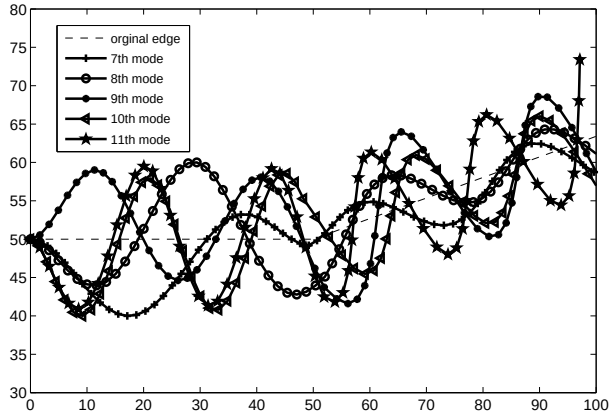

Fig. 5 The comparison of higer mode shapes

Elem., **25** (2001), pp. 581-591.

(11) J.Y. Xiao, L.H. Wen and J. Tausch, On fast matrix-Cvector multiplication in wavelet Galerkin BEM, *Eng. Anal. Bound. Elem.*, **33** (2009), pp. 159-167.

(12) J.Y. Xiao and J. Tausch, A fast wavelet-multipole method for direct BEM, *Eng. Anal. Bound. Elem.*, **34** (2010), pp. 673-679.

(13) J. Ravnik, L. Škerget and Z. Žunič, Comparison between wavelet and fast multipole data sparse approximations for Poisson and kinematics boundary - domain integral equations, *Comput. Methods Appl. Mech. Engrg.*, **198** (2009), pp. 1473-1485.

(14) X.F. Chen, S.J. Yang, Z.J. He and J.X. Ma, The construction of wavelet finite element and its application, *Finite Elem. Anal. Des.*, **40** (2004), pp. 541-554.

(15) J.W. Xiang, X.F. Chen, Z.J. He and H. B. Dong, The construction of 1D wavelet finite elements for structural analysis, *Comput. Mech.*, **40** (2007), pp. 325-339.

(16) J.W. Xiang, X.F. Chen, Y.M. He and Z.J. He, The Construction of plane elastomechanics and Mindlin plate elements of B-spline wavelet on the interval, *Finite Elem. Anal. Des.*, **42** (2006), pp. 1269-1280.

(17) J.G. Han, W.X. Ren and Y. Huang, A spline wavelet finite element method in structural mechanics, *Int. J. Num. Meth. Engng.*, **66** (2006), pp. 166-190.

(18) E. Quak and N. Weyrich, Decomposition and reconstruction algorithms for spline wavelets on a bounded interval, *Appl. Comput. Harmon. A.*, **3**(1994), pp. 217-231.

(19) J.C. Goswami, A.K. Chan and C.K. Chui, On solving first-kind integral equations using wavelets on a bounded interval, *IEEE T. Antenn. Propag.*, **43**(1995), pp. 614-622.

(20) X.C. Wang, *The Finite Element Methods*, TsingHua University Press, Beijing, 2002. (In Chinese)